

Towards the general application of water calorimetry as absorbed dose standard for radiotherapy dosimetry

A. Krauss, M. Bambynek, H.-J. Selbach

Physikalisch-Technische Bundesanstalt, Bundesallee 100, 38116 Braunschweig

Abstract

After the implementation of a water calorimeter as a primary standard for absorbed dose to water, D_W , in ^{60}Co radiation, efforts are being made at PTB to extend the application possibilities of water calorimetry for radiotherapy dosimetry in various irradiation conditions and in various radiotherapy beams. In addition to the determination of D_W in high-energy photon- and electron radiation, this covers also the application in 70 kV, 100 kV and 150 kV medium energy x-rays, in a scanned 280 MeV carbon ion beam and in close proximity to a 350 GBq ^{192}Ir -brachytherapy source, respectively. For the latter-mentioned applications, first experiments performed with different water calorimeters are presented and emphasis is placed on discussing the heat conduction effects occurring during the different measurements.

Key Words: water calorimetry, heat conduction, medium energy x-rays, ^{192}Ir brachytherapy source, scanned carbon ion beam

1. Introduction

The absorbed dose to water, D_W , is the measurement quantity of main interest in the dosimetry for radiotherapy and it is consequently applied for all types of therapeutically used ionizing radiation ranging from x-rays, over high-energy photon- and electron radiation, to proton- and heavy ion beams [1]. In practice, D_W has to be determined also for various geometric irradiation conditions and for various treatment techniques, like brachytherapy treatment or conformal radiotherapy treatment. Recent developments in conformal treatment have increased the demand for the determination of D_W especially in very small radiation field sizes.

D_W is determined in clinical dosimetry by means of ionization chambers which have been calibrated in terms of absorbed dose to water under reference conditions in ^{60}Co radiation by help of a corresponding primary standard. The various deviations of the real irradiation conditions from the reference conditions during the calibration are accounted for by applying different correction factors, for example for the energy-dependent response of the ionization chamber or for the chamber-dependent perturbation of the radiation field. The achievable uncertainty in the measurement of D_W in clinical dosimetry is dominated by the uncertainties of the values of some of these correction factors which are determined mainly with the aid of ionization chamber theory and with Monte-Carlo calculations. If standards for absorbed dose to water were available not only for ^{60}Co radiation but for all different types of ionizing radiation and for various irradiation conditions, D_W could be determined in clinical dosimetry with lower uncertainties than today, because either the correction factors mentioned could be determined experimentally or the ionization chamber could be directly calibrated for the required beam quality and for the required irradiation condition.

Water calorimetry can be applied to achieve this goal as it is the most direct method to determine D_W and because it is, on principle, an energy-independent method. At PTB, besides the primary standard water calorimeter for the determination of D_W in ^{60}Co -radiation for reference conditions [2,3], additional water calorimeters are in operation [4] to extend the possible application of water calorimetry as absorbed dose standard for various non-reference conditions. This covers the area of different beam qualities, such as high-energy photon- and electron radiation, but also the area of smaller radiation-field sizes. Furthermore, efforts are being made at PTB to apply water calorimetry for the determination of D_W in medium energy x-rays, in a scanned beam of high-energy carbon ions and in close proximity to an ^{192}Ir -brachytherapy source, respectively. As far as the latter-mentioned applications are concerned, only few experiences have so far been reported in previous publications for the cases of medium energy x-rays [5-8] and carbon ion beams [9], and no calorimetric work at all has been performed so far with regard to brachytherapy sources.

As a prerequisite for the application of water calorimetry as absorbed dose standards for the determination of D_W in the above-mentioned radiation fields, investigations similar to those which have been performed for ^{60}Co radiation -regarding the different influence quantities affecting the measurement signal of the water calorimeter- are required [2]. However, in the case of the new calorimetric applications, it is expected that some of the corresponding corrections will be significantly larger now, especially for the heat conduction effects occurring during and after an irradiation. This is due to the fact that the dose gradients at the point of measurement will partly be much steeper (which is the case especially for the point-like irradiation field of the brachytherapy source) and because of the different interaction coefficients of the radiation with the detector materials of the calorimeter which holds true especially for medium energy x-rays.

This report presents first calorimetric experiments performed in medium energy x-rays with tube voltage of 70 kV, 100 kV and 150 kV, in a scanned 280 MeV carbon ion beam and in the radiation field of a ^{192}Ir -source, respectively. The origin of different heat conduction effects occurring in these experiments is discussed and preliminary determinations of the corresponding corrections performed on the basis of heat transport calculations are presented.

2. Set-up of water calorimeters and experimental procedures

2.1 Basic set-up of calorimeters and calorimetric detector

The different water calorimeters available at PTB have already been described in detail [2,4]. Briefly, all calorimeters are operated at a water temperature of 4 °C and are designed for horizontally directed radiation beams. Each calorimeter uses mainly identical components as, for example, the cubic water phantom with an edge length of 30 cm or the calorimetric detector. However, a significant difference between the calorimeters can be found in the temperature stabilization system. The so-called primary standard water calorimeter (figure 1) is placed within an almost cubic outer container with an edge length of about 1 m, in which the temperature of 4 °C is achieved by means of temperature regulated circulating air. In the case of the so-called transportable water calorimeter (figure 2), which offers a more compact design, the temperature stabilization is achieved by means of actively cooled aluminium plates surrounding the water phantom of the calorimeter.

The calorimetric detector consists of a thin-walled plane-parallel glass cylinder filled with high-purity water saturated with hydrogen gas. The calorimetric detector can be fixed at different water depths in relation to the entrance window of the phantom and is mounted such that the axis of the radiation field coincides with the cylinder axis. Inside the cylinder, two conically shaped glass pipettes are mounted perpendicularly to the cylinder axis and opposite each other, such that the tips of the pipettes are separated by about 4 mm from the central axis of the radiation field. The tip of each pipette contains a thermistor sensor 0.25 mm in diameter directly fused into glass [2]. Inside the air-filled part of the pipette, the 30 μ m diameter Pt/Ir-wires of the thermistor are soldered to isolated copper wires of 25 μ m diameter to make the electrical connection to the signal cable of the calorimeter .

2.2 Set-up and procedures for medium energy x-rays and high-energy carbon ions

The transportable water calorimeter was applied for experiments performed with medium energy x-rays as well as for measurements performed in a 280 MeV scanned carbon ion beam.

The x-ray measurements were performed at PTB using the transportable water calorimeter which was adjusted in front of a voltage-stabilized x-ray generator of 150 kV maximum tube voltage. Measurements were made at 70 kV, 100 kV and 150 kV tube voltage with absorbed dose rates between 0.19 Gy/min and 0.33 Gy/min. The characterization of the therapy x-ray qualities are given in table 1. The distance between the focal spot of the x-ray tube and the surface of the water phantom amounted to 50 cm and the detector was placed inside the water phantom of the calorimeter at a water depth of 50 mm. At this depth, the radiation field offered a diameter of slightly more than 15 cm. The irradiation time for each beam quality amounted to 122 s and typically, series of eight successive irradiations with drift periods of 125 s in between were performed before the calorimeter had to be newly conditioned.

The heavy-ion experiments were performed at the “Gesellschaft für Schwerionenforschung” (GSI) in Darmstadt with a 280 MeV carbon ion therapy beam during one of the patient-treatment beam times. The carbon beam is guided horizontally from the heavy-ion synchrotron to the treatment room within a beam line of more than 150 m. Due to the extraction method, the ions exit the synchrotron in spills of about 2 s duration. The time interval between successive spills amounts also to about 2 s. By help of the intensity-controlled raster scan method, nearly every desired dose distribution can be achieved [10].

The transportable water calorimeter was installed in the treatment room at GSI in such a way that the iso-centre of the therapy beam coincided with the measurement point of the detector at a water depth of 50 mm. This way, the calorimetric measurements were performed in the plateau region of the corresponding depth dose distribution of the 280 MeV carbon beam. The position of the Bragg-peak of the 280 MeV beam has a depth in water of about 15 cm. The irradiation conditions were chosen to achieve a good homogeneity regarding the lateral dose distribution. Therefore, a focus diameter of the carbon beam of about 9 mm (Fwhm) was used to scan a field size of nearly 50 mm \times 50 mm within 169 discrete scan points distributed over 13 rows and 13 columns and the distance from one scan point to the next being about 3.9 mm. Each scan was repeated 12 times, but the starting position of every second scan was shifted by about 2.0 mm in both directions with respect to the very first scan. The whole scanning process resulted in a total irradiation time of about 120 s and an absorbed dose of about 2.4 Gy. Again, series of eight successive measurements were performed during the whole experiment.

2.3 Set-up and procedures for measurements with ^{192}Ir -brachytherapy source

The commercially available ^{192}Ir -HDR brachytherapy source (half time: 73.824 days) used for the calorimetric experiments offered an activity of 352 GBq at the starting time of the measurements. The source has a diameter of 0.6 mm and a length of 3.5 mm and is contained in a stainless steel encapsulation of 1.1 mm outer diameter and 5 mm length. The encapsulation, again, is welded at the tip of a long stainless steel wire of also 1.1 mm outer diameter. By help of an afterloader, the wire can be moved through a teflon catheter to the desired irradiation position.

For the calorimetric experiments with the brachytherapy source, a former version of the primary standard water calorimeter including its large outer container were somewhat modified to ensure that the source could be positioned in front of the detector cylinder inside the water phantom of the calorimeter. The afterloader is placed closely beside the outer container of the calorimeter and its long teflon catheter (1.7 mm outer diameter, wall thickness 0.25 mm) is guided through the wall of the outer container to finally reach the lid of the calorimeter housing and to enter the water phantom in vertical direction. At the inner wall of the outer container, the teflon catheter passes through a massive lead block with the dimensions 10 cm \times 10 cm \times 20 cm. This block is placed between two of the heat exchangers which are used for keeping the air temperature within the outer container of the calorimeter at a temperature of 4 °C [2]. During the calorimetric measurements, the afterloader moves the ^{192}Ir -source from its position inside this shielding block to its measurement position in front of the detector and vice versa, so that the temperature of the source itself stays permanently at 4 °C. When the ^{192}Ir -source is kept inside the lead block, the dose rate is reduced by a factor of about 1000.

Inside the water phantom of the calorimeter, the teflon catheter is connected to a stainless steel tube of about 150 mm length having a 1.6 mm outer diameter and a wall thickness of 0.15 mm. The closed end of the stainless steel tube stops the movement of the source when it is pushed into the measurement position. The stainless steel tube is fixed in vertical direction in front of one of the flat walls of the detector cylinder such that the centre of the source is located at a distance of nominally 30 mm to each of the thermistors. Prior to the irradiation measurements, the exact distance to the thermistors was determined by use of an optical telescope to be 29.4 mm and 29.42 mm, respectively.

The reproducibility of the afterloader transport mechanism was investigated in detail with the aid of a dummy source having the same dimensions as the radioactive ^{192}Ir -source and by help of photodiodes placed at certain positions along the teflon catheter. This way, the exact position of the source as well as the time needed for moving the source between the shielding block and the measurement position in front of the detector could be measured. Irradiation measurements were performed for nominal irradiation times of 90 s, 120 s and 200 s. The dose rate at the point of measurement was about 0.8 Gy/min. During the experiments, the water calorimeter was newly conditioned after each irradiation.

2.3 Data acquisition

Usually, the measurement signals of the water calorimeters at PTB are recorded by use of a dc-powered resistance bridge. For the measurements described in this report a more direct

data acquisition method was applied which fulfilled the demand for simpler operation and for higher flexibility. This acquisition system consists mainly of two high-stability digital multimeters (HP 3588A) which can be operated in different ways.

For the measurements with the brachytherapy source the resistance of each thermistor of the detector was measured separately in the direct resistance mode of the multimeters. As the thermistors principally are located at different points of measurement, possible deviations of the dose distribution from the assumed rotational symmetry can be detected this way. Using the multimeters in the direct resistance mode leads to a power dissipation in each of the thermistors of about $100 \mu\text{W}$, which is significantly larger than the $15 \mu\text{W}$ usually used in calorimetric experiments when the common resistance bridge technique is applied [2]. It should be noted that in this case the equilibrium temperature of the thermistors is about $0.12 \text{ }^\circ\text{C}$ higher than the temperature of the surrounding water and that the measured radiation-induced temperature rise has to be corrected by about -0.5% due to the change of the power dissipation during irradiation.

For all other measurements described in this report, the two thermistors of the detector were connected in series to form one part of a 1.5 V dc-powered voltage divider, the second part being a pre-resistor of almost twice the value of one of the thermistor resistances. The digital multimeters measure the voltage drop across each part of the voltage divider and in this way, the sum of the thermistor resistances is given by multiplying the precisely known resistance value of the pre-resistor with the measured voltage ratio between the thermistors and the pre-resistor. Detailed investigations showed that the signal-to-noise ratio in this operational mode is significantly lower than in the direct resistance mode. However, the signal-to-noise ratio of the common resistance bridge technique is still better by a factor of about two.

3. Preliminary results and data analysis

3.1 Medium energy x-rays

3.1.1 Experimental findings

A total of about 550 measurements were performed with the transportable water calorimeter for three therapy x-ray qualities with 70 kV , 100 kV and 150 kV tube voltage, respectively (see table 1). So far, no definite results for the determination of D_w can be given, because the detailed analysis of the various required corrections is still going on.

Figure 3 shows an example of a 122 s irradiation with 150 kV x-rays starting at $t = 0 \text{ s}$. A pronounced step in the time evolution of the calorimeter signal occurs at the beginning and at the end of the irradiation, whereas the almost linear increasing part of the signal indicates the temperature rise (measured as the resistance change of the thermistors) of the water at the point of measurement. Similar effects were observed for the other beam qualities also. For the three beam qualities the percentage ratio of the step to the total measurement signal varies between 16% and 19% , see table 2. The given ratios were determined in two steps. First, by using the common method of analyzing a calorimetric measurement, i.e. extrapolating the linear fits of the pre- and post irradiation drift curves to the middle of the irradiation and calculating the corresponding resistance change at this time. Second, by additionally performing a linear fit over a certain time interval of the signal during irradiation and calculating the resistance differences to the pre- and post irradiation drifts at the beginning and at the end of the irradiation. Essentially no variation was found between this difference at

the beginning and at the end of an irradiation. For the pre- and post-irradiation drifts, time intervals of 110 s each were used with the pre-irradiation drift interval starting 10 s after the end of an irradiation [2]. The same time interval beginning 10 s after the start of an irradiation was applied for the linear fit of the irradiation signal.

It must be considered that the step just at the end of an irradiation might still have a strong influence on the post-irradiation drift curve of the caloric measurement and therefore on the correct determination of D_w .

3.1.2 Investigation of heat conduction effects

The presence of a step occurring at the beginning and at the end of an irradiation is, as a matter of principle, caused by a heat conduction effect due to the interaction of the radiation with the non-water materials of the temperature probes of the calorimetric detector. Compared to water, the values of both the radiation interaction coefficients and the specific heat capacities of such materials deviate from those for water. The resulting influences on the determination of D_w have already been investigated in detail for the common applications of water calorimetry in ^{60}Co radiation. Depending on the real geometry of the temperature probes, corrections in the range of a few 0.1 % must typically be considered [2]. However, in the case of medium energy x-rays a much stronger effect has to be expected and in a previous investigation this had been noticed, but without determining the corresponding corrections [6].

The geometry of the temperature probes used in the PTB calorimeters have already been described elsewhere [2] and is briefly summarized in section 2.1. In the case of the measurements reported here, the tip diameter of the glass pipettes amounted to 0.72 mm. For this geometry, the ratio of the mean absorbed doses in the different materials to that in water were calculated by the Monte-Carlo method. However, such calculations require the knowledge of the thermistor material, which is typically designated as oxide alloys of different transition metals, mainly manganese. The alloy $\text{Cu}_{0.84}\text{Mn}_{2.16}\text{O}_4$, for example, is one possible thermistor composition [11]. This composition was used for the Monte-Carlo calculations and its density was estimated to be 4 g/cm^3 , which was concluded from measuring the weight of the thermistor. Within the EGSNRC-program, that part of the temperature probes which contains the thermistor was approximated in rotational symmetry including the Pt-wires of the thermistor. Additional calculations were performed to calculate the mean absorbed doses also in the air-filled part of the pipette and in the copper wires. The three different x-ray beam qualities were considered within the calculations on the basis of continuous photon fluence spectra, which were obtained from the measured pulse-height spectra by using a deconvolution method to avoid artefacts [12]. Table 3 summarizes the results of the Monte-Carlo calculations. The number of histories for the Monte-Carlo calculations were generally chosen to achieve a statistical uncertainty of less than 1 %.

The Monte-Carlo calculated ratios of the mean absorbed doses in the different materials have thus been used as the heat generation rates relative to those in water for the adjacent heat conduction calculations. The heat transport effects occurring in the temperature probes during and after a 122 s irradiation with the different x-ray qualities were calculated by the finite-element method using a model of the thermistor probe with rotational symmetry in which the two $30\text{ }\mu\text{m}$ Pt wires were combined to one wire with a correspondingly larger diameter. The results of such calculations are typically expressed as the so-called excess temperature, which is the relative ratio of the temperatures with and without heat conduction effects. The time

evolution of the calculated excess temperature is dominated by the effect of the temperature probes during the first 10 or 20 seconds after the end of an irradiation. At later times, also other heat conduction effects influence the excess temperature, namely due to the irradiation of the glass cylinder of the detector or due to the depth and lateral dose distributions inside the water phantom. Therefore, heat conduction calculations on the basis of a procedure similar to that mentioned above were also performed for these effects to finally achieve the total excess temperature.

Figure 4 shows a detail of the total excess temperature curve together with the experimental data for a 122 s irradiation with 150 kV x-rays just before and after the end of the irradiation. The excess temperature was normalized to the experimental data by help of the slope of a linear fit to the measured resistance change during the irradiation. It can be seen from the figure that first, the principal shape of the calculated decreasing part of the step after the end of the irradiation is in agreement with the data, and second, that the height of the calculated jump is only about 60 % of the jump in the measurement. This finding is nearly the same also for the irradiations with 70 kV and 100 kV x-rays, see table 1. A closer view of the result of the heat conduction calculations shows that roughly 50 % of the calculated step is caused by the irradiation of the small Pt wires of the thermistors. A variation of the heat generation rates in the wires of about 20 % changes the resulting height of the step by about 10 %. Similar variations have also been made for other parameters used within the calculations, but so far, the observed discrepancy between the experimental and the calculated step could not be reasonably resolved by such variations.

In principle, not the height of the step but the time-dependent decrease of the step after the irradiation is important for a correct determination of D_w . As mentioned in section 3.1.1, D_w is determined from the experimental data by performing linear fits to the pre- and post irradiation drift curves over certain time intervals. The required correction factors for the heat conduction effects are deduced from the calculated excess temperature using the same linear fit method. This way, for the irradiations with 70 kV, 100 kV and 150 kV x-rays, the mean heat conduction correction factors for a set of 8 consecutive measurements amount to about 3 % with only small variations for the different beam qualities. The corrections for the first measurement within such a series of eight irradiations are typically about 1.5 % lower.

3.1.3 Investigation of additional effects

To find the possible cause of the discrepancy between the observed and the calculated step, investigations were carried out by replacing the temperature probes of the calorimetric detector against isolated wires of copper or platinum, respectively. The thermistor resistances were replaced by two 10 k Ω resistors within the measurement circuit of the voltage divider. It was observed that the measured resistance of the “detector” decreased by a fraction of about 3×10^{-7} and recovered simultaneously when the 150 kV radiation was switched on and off. The reason for this was found to be associated with the connection box of the calorimetric detector in which the signal cable of the calorimeter is soldered to the leads of the temperature probes. Although the box is located outside the radiation field above the water phantom of the calorimeter, the dose rate of scattered x-rays is high enough to produce a small current between the leads of the “detector” due to the ionization of the air inside this box. For measurements in ^{60}Co radiation this “ionization”-effect is almost negligible because of the much smaller fraction of scattered photons.

It is deduced that the “ionization”-effect has caused an almost constant resistance change of about 5.5 mΩ during the x-ray measurements with the calorimetric detector. This is equivalent to a contribution to the observed ratio of step to signal of about 0.05 in the case of the 100 kV and 150 kV measurements and of about 0.08 in the case of the 70 kV measurements, respectively. These results are also given in table 2.

In the case of the temperature probes, an ionization current might also occur between the bare Pt leads of the thermistors. Because they are surrounded by air over a length of a few mm within the very thin part of the glass pipette only, the effect of the ionization of the air during irradiation should be small and is roughly estimated to possibly contribute about 0.01 to the observed step-to signal-ratio.

3.2 ¹⁹²Ir brachytherapy source

3.2.1 Experimental findings

A total of about 300 measurements have been performed so far for nominal irradiation times of 90 s, 120 s and 200 s. Figure 5 offers an example of a set of three measurements performed on the same day with different irradiation times. It can be seen that the corresponding post-irradiation drift curves for the different irradiation times begin to strongly increase some time after the end of the irradiation. For the 200 s irradiation this effect is much more pronounced than for the 90 s irradiation. It must be concluded that the determination of D_W will be difficult in the case of the 200 s irradiation if the common method of performing linear fits to the pre- and post irradiation drift curves is applied. Without correction, this method would underestimate the radiation induced resistance change of the thermistor by about 30 %. Although the situation seems to be much better in the case of the 90 s and 120 s irradiations, the underlying effects which influence the post-irradiation drift curves have to be understood and have to be finally corrected in any case.

3.2.2 Heat conduction effects

During the radioactive decay of ¹⁹²Ir, photons of various energies with the main emissions centred at energies around 300 keV and around 470 keV as well as a broad spectrum of low-energy electrons are emitted [13]. The electrons are mainly absorbed within the source material or within the stainless steel encapsulation of the source. Nevertheless, both types of radiation lead to heat conduction effects inside the water phantom of the calorimeter and will therefore influence the calorimetric measurements.

The heat transport effects were investigated by help of finite-element calculations using a model of the ¹⁹²Ir source located within the stainless steel tube of the end of the catheter at a distance of 29.4 mm in front of the calorimetric detector. In a first step, a rotational symmetric model was used to study only those effects which are caused by the heat transport in water, i.e. the influence of the irradiation of the materials of the detector itself was omitted. The depth dose distribution of the photon radiation field which approximately follows an $1/r^2$ -function, where r is the radial distance from the centre of the source, was calculated via Monte-Carlo calculation. The heat generation rates to be used within the calculations were deduced for the photon field from the measured slope of the temperature change during the 90 s irradiations. In addition, the rate of the self-heating of the source caused by the absorption of the electrons and photons is required. The fraction of photons was obtained by

help of Monte-Carlo calculations using a corresponding model of the source together with its encapsulation. The fraction of electrons was calculated by using the known β - and Auger-spectrum of ^{192}Ir and the assumption that the electrons are completely absorbed in the source and the encapsulation. This way, the rate of the self-heating of the source, having an activity of 352 GBq, was calculated to be 18.5 mW with a relative standard uncertainty of 10 %. For the finite-element calculations it was taken into account that the dose rate of the photon field and the self-heating of the source must relate to the same date. It was assumed that the temperature of the source stayed constant during the movement of the source into its measurement position via the afterloader.

The calculations show that the temperature at the centre of the source is about 1.1 °C higher than the operating temperature of the calorimeter at the end of a 90 s irradiation. This is largely independent of the exact value of the assumed constant temperature during the movement of the source. The heat conduction caused by the temperature difference between source and water influences the shape of the post-irradiation drift curves of the calorimetric measurements, especially in the case of the 200 s irradiation. Figure 6 shows a comparison of the experimental data with the result of the heat conduction calculations in case of a 90 s irradiation. The calculated excess temperature was normalized to the experimental data by help of the slope of a linear fit to the measured resistance change during the irradiation. A good agreement between experiment and calculation is achieved for the post-irradiation drift curve over more than 250 s. The situation differs in case of the 200 s irradiation which is partly shown in figure 7. The dashed line is the calculated result using the same set of independently achieved information for the dose rate and the self-heating rate, respectively, as it was used for the 90 s calculation, whereas for the solid line the dose rate was increased by about 6 %. In the latter case, the agreement between experiment and calculation is much better.

These results indicate that the time dependence of the calorimetric measurements can be principally understood on the basis of the simple model calculations presented here. More detailed calculations have to consider the real 3-dimensional dose distribution in the water phantom as well as the influence of the detector materials.

3.3 Scanned carbon ion beam

3.3.1 Experimental findings

About 70 calorimetric measurements were performed with a scanned carbon ion beam of 280 MeV. The irradiation conditions are described in section 2.2. Figure 8 demonstrates the calorimetric signal for one of these measurements and it can be seen that 12 steps occur during the time of the irradiation. These steps correspond to the scanning of the beam across the calorimetric detector, because each time the beam reaches the vicinity of the thermistors a strong temperature increase is measured. The overshooting, which can be seen in the figure for almost each step, might be caused by the direct radiation interaction with the material of the temperature sensor. On principle, each step should also offer a “fine-structure” of some smaller steps, but the data acquisition rate of the calorimeter was not high enough to resolve this structure.

3.3.2 Heat conduction effects

For the investigation of the heat conduction effects occurring in this experiment it is essential to consider the exact time evolution of the irradiations, i.e. the duration of one spill and the time interval between the spills. Work is in progress to take this into account within the corresponding finite-element calculations. Because the depth dose distribution at the point of calorimetric measurement is very smooth, the calculations can be performed on the basis of a two-dimensional model. Without considering the spill structure of an irradiation, previous calculations in the case of more ideal irradiation conditions showed that the corresponding heat conduction corrections amount to less than 0.2 % [4]. Future calorimetric experiments are planned to be carried out directly at a spread-out Bragg peak of a scanned carbon ion beam. In this case, the time-dependent finite-element calculations have to be performed for a full 3-dimensional model, similar to how it was done previously in the case of a scanned proton beam [13].

4. Conclusions

At PTB, work is in progress to apply water calorimetry as absorbed dose standards to a wide variety of different radiotherapy beams. This report shows that the determination of D_W in the case of medium energy x-rays, in the case of scanned carbon ion beams and in the case of a ^{192}Ir brachytherapy source can, on principle, be performed with the different water calorimeters available at PTB. However, the extensive investigation of influence quantities, for example heat conduction effects occurring during and after an irradiation, is an essential prerequisite before a sound uncertainty budget for the determination of D_W can be achieved. For the different types of radiotherapy beams mentioned here, the origin of heat transport effects has been discussed and some preliminary results for the required corrections could be given. These investigations will be completed in the near future.

A further important influence quantity in water calorimetry is the so-called heat defect. The heat defect which might change the energy balance between the absorbed energy and the energy appearing as heat, must be especially considered in the case of the scanned carbon ion beam, because the linear energy transfer (LET) for this type of radiation is different from that of photon- or electron radiation and furthermore, the dose rate per scan point is very high. Although theoretical considerations on the basis of the LET dependency of the radiolysis of water suggest that there should be no deviation for water saturated with hydrogen, experimental work still has to be performed on this subject to support the theoretical expectation.

References

- [1] IAEA TRS-398, 2000, *Absorbed dose determination in external beam radiotherapy: an international code of practice for dosimetry based on standards of absorbed dose to water*, IAEA, Vienna, ISBN 92-0-102200
- [2] Krauss A 2006 *Metrologia* **43** 259-272
- [3] Kessler C, Allisy P J, Burns D T, Krauss A and Kapsch R-P 2006 *Metrologia* **43** Tech. Suppl. 06005
- [4] Krauss A 2006 *Thermochim. Acta* **445** 126-132
- [5] Mattson O 1988 *Proc. NRC Workshop on Water Calorimetry (Ottawa)* ISBN 0-660-12942-6, 17-24
- [6] Seuntjens J, Thierens H, Poffyn A and Segaeert O 1988 *Proc. NRC Workshop on Water Calorimetry (Ottawa)* ISBN 0-660-12942-6, 101-107
- [7] Seuntjens J, Thierens H and Schneider U 1993 *Phys. Med. Biol.* **38** 805-832
- [8] Damen P and de Prez L 2005 *Biomedizinische Technik 50 Suppl. Vol. 1 Part 1*, 261-262
- [9] Brede H J, Greif K D, Hecker O, Heeg P, Heese J, Jones D T L, Kluge H and Schardt D 2006 *Phys. Med. Biol.* **51** 3667-3682
- [10] Haberer T, Becher W, Schardt D and Kraft G 1993 *Nucl. Instrum. Methods B* **139** 58
- [11] Kukuruznyak D A, Ahmet P and Chikyow T 2005 *J. Appl. Phys.* **98** 043710
- [12] Schneider T and Kramer H-M 2006 *Radiat. Prot. Dosimetry* **121** 370-375
- [13] NCRP Report 58, 1985, *A Handbook of Radioactivity Measurements Procedures*, NCRP Publications, Bethesda MD. 20814, ISBN 0-913392-71-5
- [14] Sassowsky M and Pedroni E 2005 *Phys. Med. Biol.* **50** 5381-5400

Tables

Table 1. Characterization of the therapy x-ray qualities used in the calorimetric experiments

Tube voltage	Filtration	Half-value layer
70 kV	4 mm Al	3.11 mm Al
100 kV	4.5 mm Al	4.52 mm Al
150 kV	4.0 mm Al 0.5 mm Cu	11.1 mm Al

Table 2. Experimental and calculated step to signal ratio occurring in the medium energy x-ray measurements due to the irradiation of the temperature probes. In addition, the estimated contribution caused by the ionization of air inside the connection box of the detector is given.

Tube voltage	Step / Signal		
	<i>Experimental</i>	<i>Calculation</i>	<i>“Ionization”</i>
70 kV	0.18 ± 0.06	0.12	0.08
100 kV	0.19 ± 0.06	0.11	0.05
150 kV	0.16 ± 0.03	0.10	0.05

Table 3. Monte-Carlo calculated ratio of mean absorbed doses in different materials to that in water for different x-ray qualities.

Material	Tube voltage		
	70 kV	100 kV	150 kV
Thermistor*	32.8	29.8	21.3
Platinum	55	61	66
Pyrex	3.2	2.9	2.2
Copper	45	42	30

* $\text{Cu}_{0.84}\text{Mn}_{2.16}\text{O}_4$

Figure Captions

Fig. 1. Picture of the primary standard water calorimeter located in front of the ^{60}Co radiation facility (left part). Shown is the calorimeter's outer container as well as the coolers and some of the associated electronics. A former version of this calorimeter was used for the measurements with the ^{192}Ir -brachytherapy source.

Fig. 2. Picture of the transportable water calorimeter with the corresponding cooling unit. The calorimeter has an almost cubic shape of about 60 cm edge length. This calorimeter was used during the x-ray experiments and during the heavy-ion measurements.

Fig. 3. Measured resistance change during and after a 122 s irradiation with 150 kV x-rays. Shown is the calorimetric signal (A) and the extrapolation of the pre- and post-irradiation drift curves (B). For the figure, the initial slope of the pre-irradiation drift was normalized to zero.

Fig. 4. Detail of figure 1, showing the decrease of the step structure within the calorimetric data (A) for the 150 kV measurement after the end of the irradiation. For the figure, the initial slope of the pre-irradiation drift was normalized to zero. The calculated excess temperature (B) was normalized to the experimental data by help of the slope of a linear fit to the measured resistance change during the irradiation.

Fig. 5. Measured resistance change during and after three irradiations with the ^{192}Ir brachytherapy source. The irradiation times amounted to 90 s (C), 120 s (B) and 200 s (A), respectively. For the figure, the initial slope of the pre-irradiation drift was normalized to zero.

Fig. 6. Comparison of the experimental data (A) with the result of heat conduction calculations (B) in the case of the 90 s irradiation. For the figure, the initial slope of the pre-irradiation drift was normalized to zero. The result of the calculation was normalized to the experimental data by help of the slope of a linear fit to the measured resistance change during the 90 s irradiation.

Fig. 7. Comparison of the experimental data (A) with the result of heat conduction calculations (B and C) in the case of the 200 s irradiation. Only a part of the calorimetric signal is shown. For the figure, the initial slope of the pre-irradiation drift was normalized to zero. The same normalization factor as for figure 6 was used in the case of (C). For (B), the normalization factor was varied by about 6 % to achieve a better agreement to the experimental data.

Fig. 8. Measured resistance change during and after an irradiation with 280 MeV carbon ions. For the figure, the initial slope of the pre-irradiation drift was normalized to zero.



Figure 1



Figure 2

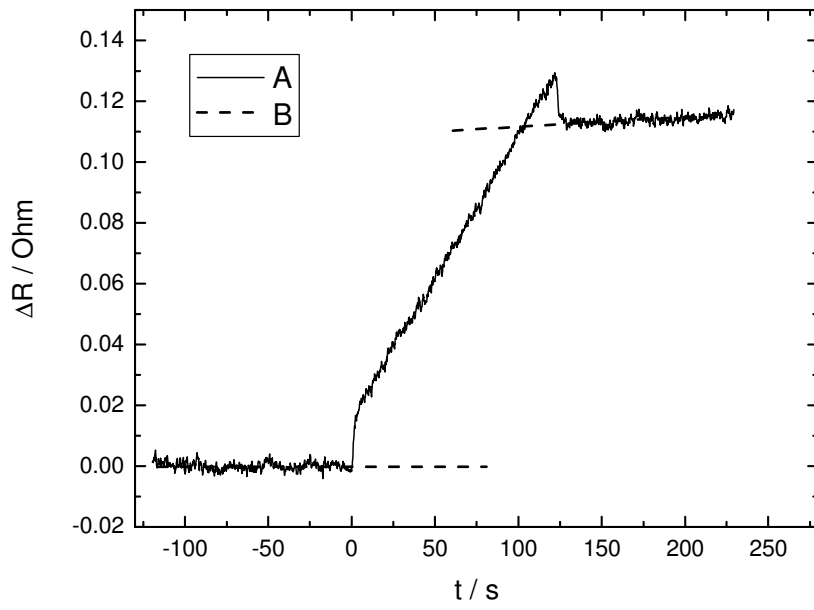


Figure 3

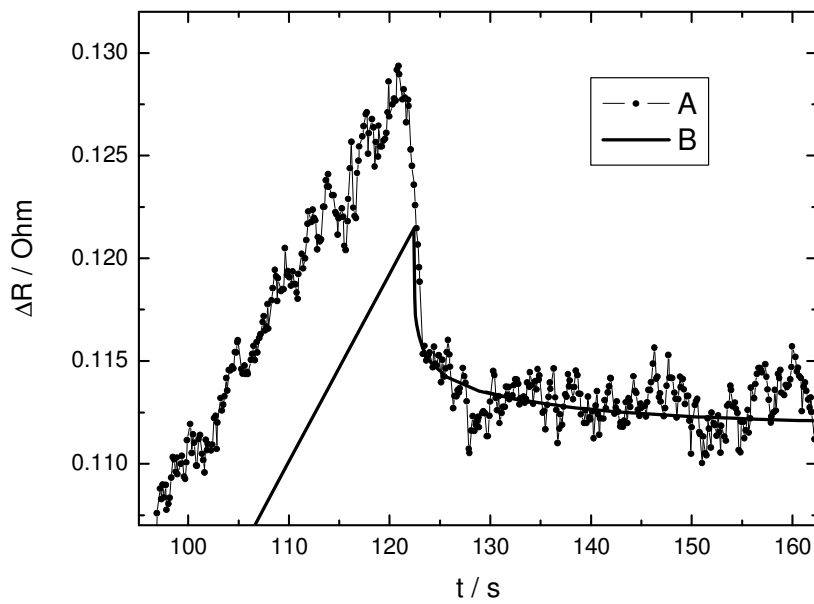


Figure 4

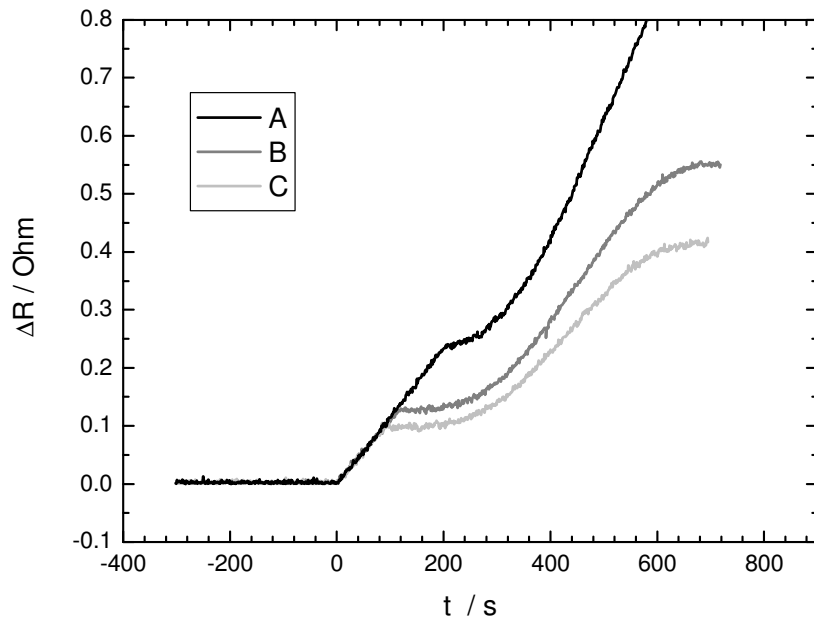


Figure 5

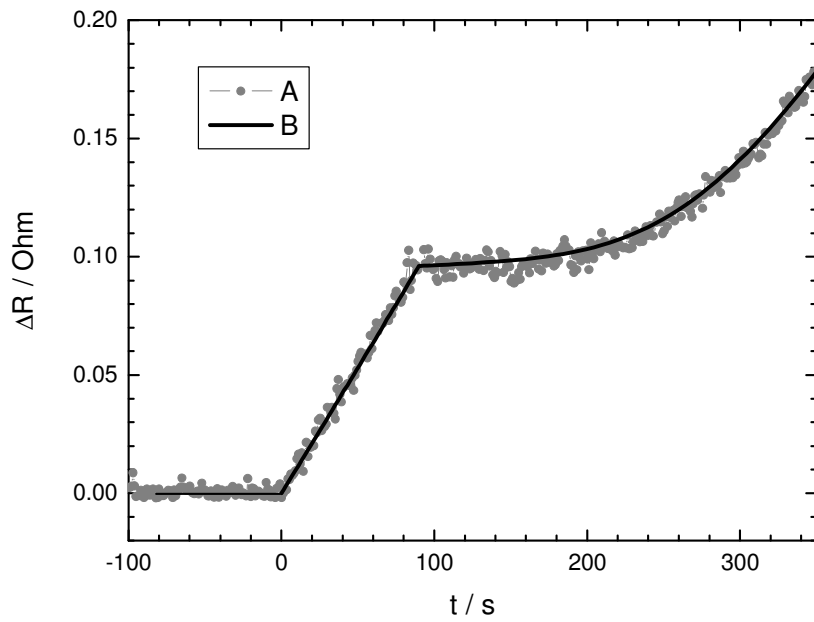


Figure 6

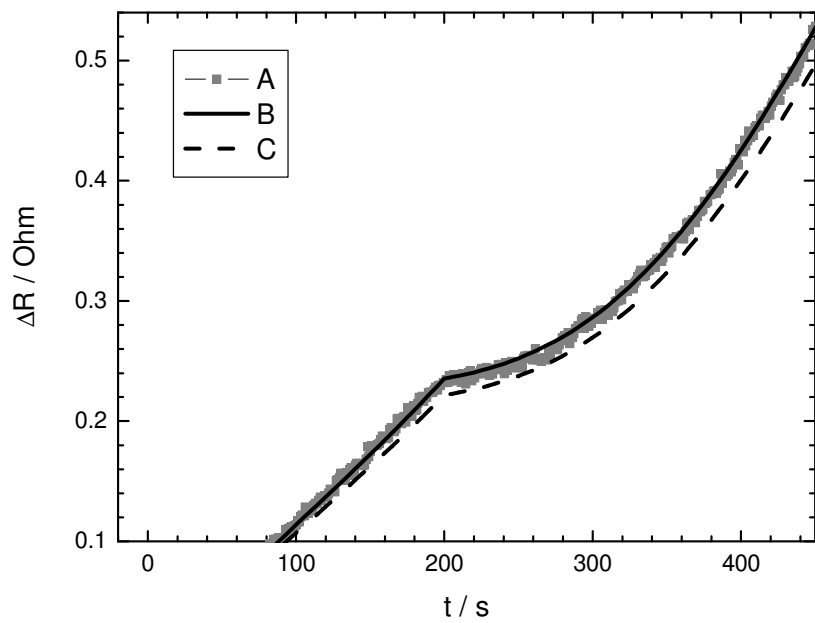


Figure 7

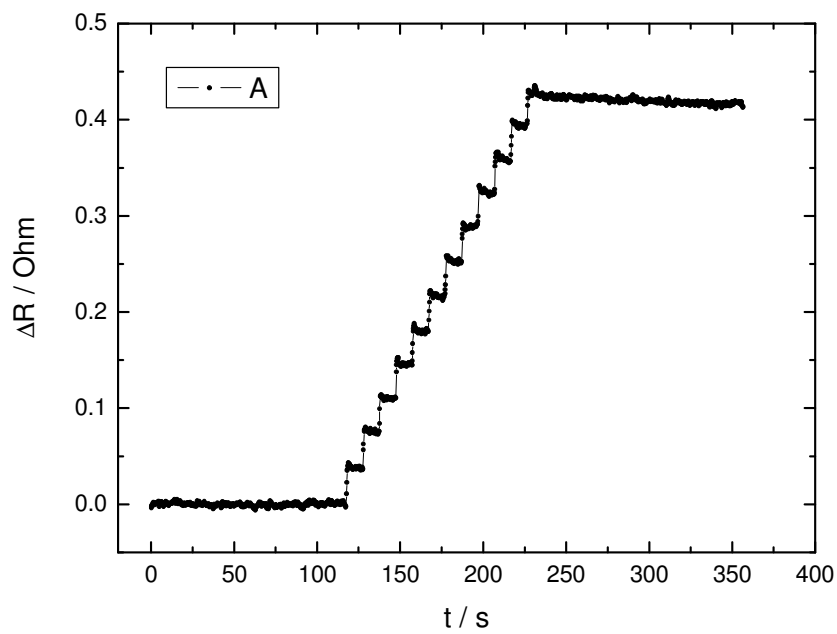


Figure 8